of their best fit which follows for the nonreduced k_D a power law of

$$k_D = 0.13 M_w^{0.43} \quad (cm^3/g) \qquad (15)$$

To obtain the reduced values, we used the relationship $R_H = 0.0229 M_w^{0.5}$ published by Schmidt et al.[30] The line for k^*_D agrees indeed satisfactorily with the high molecular weight data. Here we only wish to draw attention to the low-M_w region, where k_D apparently increases slightly with reducing M_w.

Acknowledgment. A.Z.A. expresses his gratitude to the University of Freiburg for a guest professorship that was kindly provided by the SFB 60 of the Deutsche Forschungsgemeinschaft. We thank the Deutsche Forschungsgemeinschaft for supporting this project.

Registry No. PS (homopolymer), 9003-53-6; toluene, 108-88-3.

References and Notes

(1) Flory, P. J. "Principles of Polymer Chemistry"; Cornell University Press: Ithaca, NY, 1953; p 529ff.
(2) de Gennes, P-G. "Scaling Concepts in Polymer Physics"; Cornell University Press: Ithaca, NY, 1979; P 76ff.
(3) Akcasu, A. Z.; Benmouna, M. *Macromolecules* **1978** *11*, 1193.
(4) Akcasu, A. Z. *Polymer* **1981** *22*, 1169.
(5) Barrett, A. J. *Macromolecules* **1984**, *17*, 1561.
(6) Oono, Y.; Freed, K. F. *J. Phys. Math. Gen. A: Math. Gen.* **1982**, *15*, 1931.
(7) Witten, T. A.; Schäfer, L. *J. Phys. A: Math. Gen.* **1978**, *11*, 1843.
(8) Adam, M.; Delsanti, M. *Macromolecules* **1977**, *10*, 1229.
(9) Han, C. C.; Akcasu, A. Z. *Polymer* **1981**, *22*, 1165.
(10) Huber, K.; Bantle, S.; Burchard, W.; Lutz, P. *Macromolecules* **1985**, *18*, 1461.
(11) Bantle, S.; Schmidt, M.; Burchard, W. *Macromolecules* **1982**, *15*, 1604.
(12) Yamakawa, H.; Fujii, M. *Macromolecules* **1973**, *6*, 407.
(13) Norisuye, T.; Fujita, H. *Polym. (Tokyo) J.* **1982**, *14*, 143.
(14) Johnson, R. J.; Schrag, J. L.; Ferry, J. D. *Polym. J. (Tokyo)* **1970**, *1*, 742.
(15) Ferry, J. D. "Viscoelastic Properties of Polymers", 3rd ed.; Wiley: New York, Chichester, Brisbane, Toronto, 1980; p 194ff.
(16) Raczek, J. Dissertation, Mainz, 1980.
(17) Ter Meer, H.-U.; Burchard, W.; Wunderlich, W. *Colloid Polym. Sci.* **1980**, *285*, 675.
(18) Pyun, C. W.; Fixman, M. *J. Chem. Phys.* **1964**, *41*, 937.
(19) Yamakawa, H. *J. Chem. Phys.* **1962**, *36*, 2995.
(20) Altenberger, A. R.; Deutch, J. M. *J. Chem. Phys.* **1973**, *59*, 894.
(21) Felderhof, B. U. *J. Phys. A: Math. Gen.* **1978**, *11*, 929.
(22) Harris, S. *J. Phys. A: Math. Gen.* **1976**, *9*, 1895.
(23) Batchelor, G. K. *J. Fluid Mech.* **1972**, *52*, 245.
(24) Hess, W.; Klein, R. *Physica A (Amsterdam)* **1976**, *85*, 509.
(25) This β value was obtained with the Padé approximation 5(1,1) given by Tanaka,[26] which is a relationship between z and α_S. The required α_S values were calculated, with the two relationships between $\langle S^2 \rangle^{1/2}$ and M_w in toluene and cyclohexane published in ref 10. This procedure yields z values as a function of the degree of polymerization, from which an average value of β was estimated with an error of about 25%.
(26) Tanaka, G. *J. Polym. Sci., Polym. Phys. Ed.* **1979**, *17*, 305.
(27) Varma, B. K.; Fujita, Y.; Takahashi, M.; Nose, T. *J. Polym. Sci., Polym. Phys. Ed.* **1984**, *22*, 1718.
(28) A ratio of $h^* = 0.83$ is obtained if for both solvents the Θ values for m_L and l_K are used.
(29) Tsunashima, Y.; Nemoto, N. *Macromolecules* **1983**, *16*, 1941.
(30) Schmidt, M.; Burchard, W. *Macromolecules* **1982**, *14*, 210.
(31) Mandema, Aw.; Zeldenrust, H. *Polymer* **1977**, *18*, 835.
(32) Nemoto, N.; Makita, Y.; Tsunashima, Y.; Kurata, M. *Macromolecules* **1984**, *17*, 425.
(33) Yu, T. L.; Reihanian, H.; Jamieson, A. M. *Macromolecules* **1980**, *13*, 1590.
(34) King, T. A.; Knox, A.; Lee, W. I.; McAdam, J. D. C. *Polymer* **1973**, *14*, 151.
(35) Han, C. C.; McCrackin, F. L. *Polymer* **1979**, *20*, 427.
(36) Jones, G.; Caroline, J. *J. Chem. Phys.* **1979**, *37*, 187.
(37) Huber, K.; Burchard, W.; Akcasu, A. Z. *Macromolecules*, submitted.
(38) Van den Berg, J. W. A.; Jamieson, A. M. *J. Polym. Sci., Polym. Phys. Ed.* **1983**, *21*, 2311.
(39) Cotton, J. P. *J. Phys. Lett.* **1980**, *41*, 231.
(40) Miyaki, Y.; Einaga, Y.; Fujita, H. *Macromolecules* **1978**, *11*, 1180.
(41) The h^* ratios noted do not agree with more recent exact eigenvalue calculation fits obtained by Ferry, Schrag, and coworkers for the very same data discussed in ref 14 and 15. The more complete treatment and resultant data fits suggest that the bead–spring model h^* values would be 0.06–0.1 in very good solvents such as toluene, and about 0.22–0.25 in Θ solvents. Thus the ratio quoted from the older fits, 0.6, is too large. A more reasonable value would be 0.25–0.35. See: *Faraday Symp. Chem. Soc.* **1983**, *18*, 173–188 and Lodge, T. P.; Schrag, J. L. *Macromolecules* **1982**, *15*, 1376–1384 for references to more complete evaluations of hydrodynamic interaction in the context of the bead–spring model. (We thank one of the referees for this comment.)

Small- and Intermediate-Angle Neutron Scattering from Stereoregular Poly(methyl methacrylate)

J. M. O'Reilly*

Research Laboratories, Eastman Kodak Company, Rochester, New York 14650

D. M. Teegarden[†]

Webster Research Center, Xerox Corporation, Webster, New York 14580

G. D. Wignall

NCSASR, Oak Ridge National Laboratory, Oak Ridge, Tennessee 37830.
Received December 3, 1984

ABSTRACT: Small- and intermediate-angle scattering (Q = 0.005–0.28 Å^{-1}) from amorphous poly(methyl methacrylate) (PMMA) of various stereoregularity was measured. The measured radii of gyration and characteristic ratios compare favorably with rotational isomeric state calculations (RIS). Isotactic PMMA shows a Debye-like scattering function, whereas the syndiotactic and atactic samples show a maximum in the scattering function. These results are similar to the RIS calculations for polymers of similar tacticities.

Introduction

Studies to ascertain the effect of stereoregularity on glass structure and on the physical properties of poly(methyl methacrylate) (PMMA) have been extended to include the technique of small-angle neutron scattering (SANS). Samples analyzed by this technique consist of a matrix of hydrogenous polymer molecules in which a fraction of isotopically substituted (deuterium labeled) molecules are dissolved. The difference in coherent scattering length b

[†]Present address: St. John Fisher College, Chemistry Department, Rochester, NY 14618.

0024-9297/85/2218-2747$01.50/0 © 1985 American Chemical Society

Table I
Characterization Data for PMMA

	$M_w \times 10^{-3}$	M_w/M_n	tacticity, % triads iso	hetero	syndio	X_m[a]
		H-8 Molecules				
isotactic	120		95	5	3	0.97
atactic	104	2.5		40	60	0.20
syndiotactic	83			23	77	0.11
		D-8 Molecules				
isotactic	109	2.8	98			0.98
atactic	101	2.8	6	36	58	0.24
syndiotactic	85	2.5	2	22	76	0.13

[a] X_m = fraction of meso diads.

between deuterium ($b_D = 0.66 \times 10^{-12}$ cm) and hydrogen ($b_H = -0.37 \times 10^{-12}$ cm) results in a marked contrast between the normal (hydrogenous) and labeled (deuterated) molecules and gives direct information on the chain conformation in the bulk.[1-8] SANS data were collected as a function of the scattering vector $Q = (4\pi/\lambda) \sin \theta$, where 2θ is the angle of scatter and λ is the incident wavelength. Radii of gyration (R_g), molecular weights (M_w), and characteristic ratios (C_∞) of the labeled chain were measured in the small-Q range ($QR_g < 1$), where the scattering is sensitive to the overall chain size. Measurements in the intermediate-Q range (Q = 0.05–0.3 Å^{-1}) are sensitive to the details of the local chain configuration over distances ~20–100 Å and show the effect of chain tacticity over this range.

The well-known difference in glass-transition temperature and other properties of PMMA were examined and are discussed in terms of the conformational properties of the chain as determined from SANS.

Experimental Section

The synthesis of the deuterated polymers has been described.[9] Hydrogenous polymers were prepared by the same procedure. Molecular weights were determined with a low-angle laser light-scattering photometer (Chromatrix KMX-6) coupled to a gel-permeation chromatograph.[10] Polydispersities were estimated from the chromatograms. These results are summarized in Table I.

Samples for SANS were prepared by dissolving the polymers in toluene (5% solution) and reprecipitating with methanol. Polymers were dried in a vacuum oven, and the powders were pressed into sheets ~0.2 mm thick. Disks (12-mm diameter) cut from the sheets were stacked to obtain samples for scattering (~2 mm thick). For each type of PMMA synthesized (atactic, isotactic, and syndiotactic), blends of labeled (PMMA-D) and unlabeled (PMMA-H) polymer were made at 20 wt % in addition to blank samples containing only PMMA-D or PMMA-H.

The neutron measurements were performed at the NSF-funded 30-m SANS facility[11] at the National Center for Small-Angle Scattering Research (Oak Ridge National Laboratory). For the small-Q measurements the 4.75-Å incident beam ($\Delta\lambda/\lambda$ = 6%) was collimated by source (2.0-cm diameter) and sample (1.0-cm diameter) slits separated by 7.5 m. The area detector (64 × 64 cm, with 1-cm^2 element size mounted on rails inside a 20-m vacuum flight path, was positioned 7 and 14 m from the sample to give an effective Q range of 0.005–0.070 Å^{-1}. For the intermediate-Q-range measurements, source and sample slits of 3.5- and 1.0-cm diameter were used with a sample–detector distance of 2.0 m to give an effective Q range of 0.02–0.28 Å^{-1}. In both Q ranges the scattering patterns were corrected on a cell-by-cell basis for instrumental backgrounds and detector efficiency variation, and radially averaged intensities were divided by the sample transmission (T) and thickness and normalized to a constant incident flux. Correction for the spatial variation of detector efficiency was made by dividing all measured scattering patterns by the background-corrected scattering from an isotropic scatterer (H_2O). The blank samples of pure PMMA-D and PMMA-H were also measured in both small- and intermediate-Q ranges to check for the presence of void scattering and to provide a basis for subtraction of the angular-independent incoherent scattering arising principally from ^{1}H nuclei.

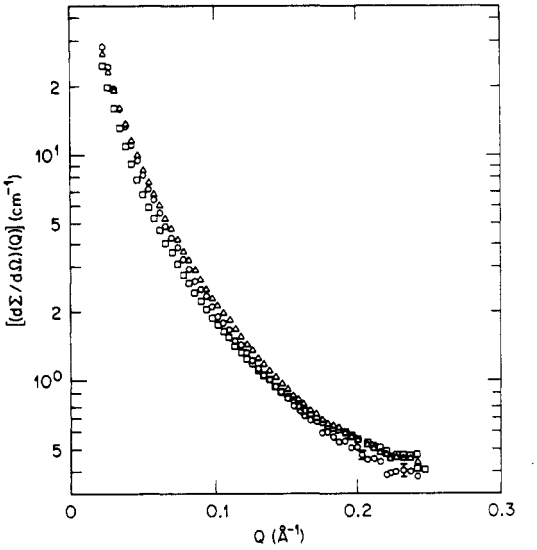

Figure 1. $(d\Sigma/d\Omega)(Q)$ vs. Q for labeled PMMA samples as a function of tacticity: (□) isotactic PMMA 2/8 (H/D); (○) atactic PMMA 2/8 (H/D); (△) syndiotactic PMMA 2/8 (H/D).

The corrected scattering patterns all showed cylindrical symmetry about the incident beam, and the measured intensities were therefore radially averaged and converted to an absolute differential scattering cross section $(d\Sigma/d\Omega)(Q)$ per unit solid angle, per unit volume of material (in units of cm^{-1}) by comparison with the scattering of secondary standards. In the intermediate-angle range, vanadium and water,[12] which show isotropic incoherent scattering, were used as standards, whereas in the small-Q range, standards of partially labeled blends of monodisperse polystyrenes[13] of known M_w and independently calibrated aluminum single crystals containing ~0.7% voids[14] were used. The overall agreement among all calibration standards was better than ±5% after scaling for the different sample–detector distances used in each Q range.

Results and Discussion

Figure 1 shows the intermediate-Q-range scattering cross section of three partially labeled blends, each containing 20 wt % (21.2 vol %) PMMA-H in a PMMA-D matrix. This ratio of labeled to unlabeled polymer, indicated by 2/8 (H/D) in Figure 1, was chosen to optimize the ratio of coherent to incoherent background scattering. Only one concentration series was measured, as it has been shown that both R_g and M_w can be obtained from a single concentration measurement if the molecular weights of the labeled and unlabeled molecules are matched. Small corrections[15] for mismatch between the labeled and unlabeled molecules were applied as described below. Figure 2 shows the apparent cross section of three PMMA-H blanks, each of which shows, predominantly, the angle-independent incoherent scattering due to the ^{1}H nuclei in the molecules. The level of scattering is a function of the sample thickness (t) and transmission (T), indicating that there is a considerable contribution due to multiple scattering, and hence the measurements do not indicate a true cross section, which is an intensive material property. However, even for thick samples with appreciable multiple scattering, the pattern is still independent of angle, and this effect forms the basis of methods used to estimate the incoherent background in the partially labeled samples. Figure 3 shows the cross section for two fully deuterated PMMA-D blanks, one of which shows appreciable angular-dependent scattering, presumably originating from voids. Although the general levels of scattering from all blanks (Figures 2 and 3) are much lower than the coherent

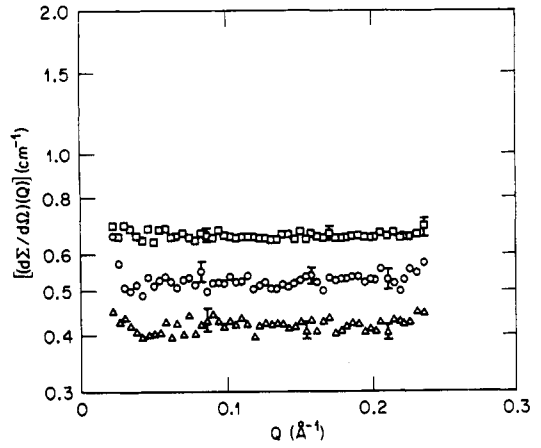

Figure 2. $(d\Sigma/d\Omega)(Q)$ vs. Q for three fully hydrogenous PMMA-H blanks: (□) isotactic PMMA-H, t = 0.12 cm, T = 0.530; (○) syndiotactic PMMA-H, t = 0.057 cm, T = 0.751; (△) isotactic PMMA-H, t = 0.020 cm, T = 0.904.

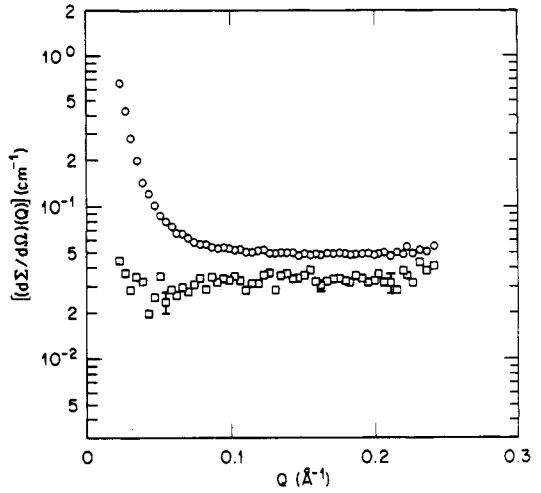

Figure 3. $(d\Sigma/d\Omega)(Q)$ vs. Q for two fully deuterated PMMA-D8 blanks: (○) syndiotactic PMMA-D, t = 0.283 cm, T = 0.808; (□) atactic PMMA-D, t = 0.069 cm, T = 0.966.

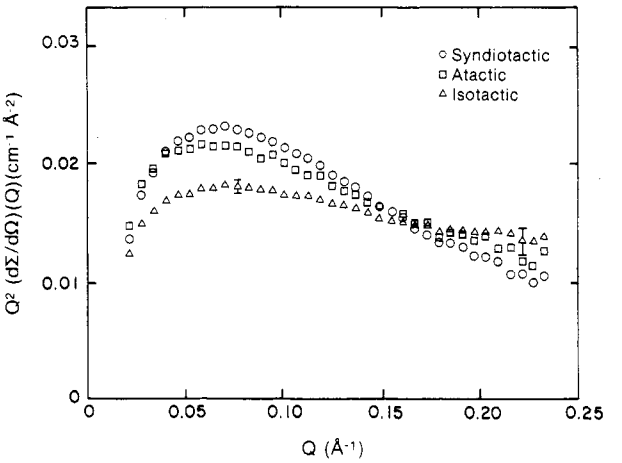

Figure 4. Intermediate-angle Kratky plots for 21.2 vol % PMMA-H molecules in PMMA-D matrix. Flat backgrounds calculated by scaling to $(1 - T)\ \sigma_{inc}/\sigma_{tot}$ according to ref 16: (○) syndiotactic; (□) atactic; (△) isotactic.

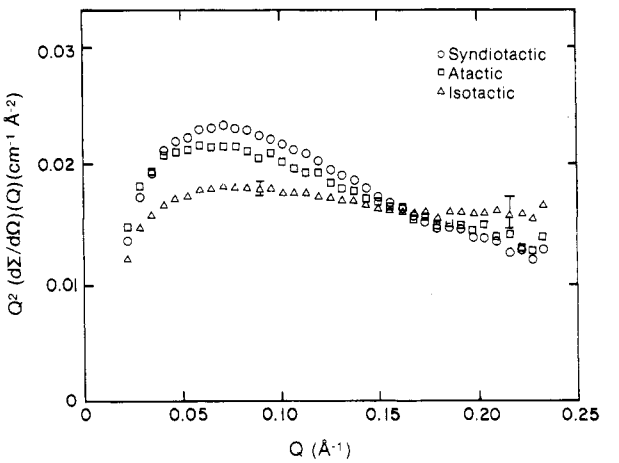

Figure 5. Intermediate-angle Kratky plots for 21.2 vol % PMMA-H molecules in PMMA-D matrix. Flat backgrounds calculated according to ref 17: (○) syndiotactic; (□) atactic; (△) isotactic.

scattering from partially labeled samples (Figure 1), subtraction of the void scattering, when present, increased the uncertainty in the M_w and R_g values for some samples calculated from the data in the low-Q range. In the intermediate-Q range the void scattering did not appreciably affect the data, and the main corrections were subtraction of the flat background levels, particularly the incoherent scattering arising from hydrogen.

As the intermediate-angle results were particularly sensitive to the background subtraction, two different methods were used to estimate this correction. For both the hydrogenous and deuterated blanks, the flat backgrounds are functions of the sample thickness and transmission (Figures 2 and 3). Studies of background scattering from H_2O/D_2O mixtures[16] showed that the flat background level was proportional to $(1 - T)$ for cells 1–2 mm thick and that the constant of proportionality for D_2O was about half that for H_2O. For intermediate concentrations the flat backgrounds could be approximately scaled to $\sigma_{inc}/\sigma_{tot}$, where σ_{inc} and σ_{tot} are the mean incoherent and total cross sections per molecule in the mixture. Similarly, the scattering from a range of hydrogenous blanks (Figure 3) of different thicknesses may be shown to be proportional to $(1 - T)$ to a good approximation, as expected for nonabsorbing samples containing predominantly incoherently scattering molecules.[12] The flat background level from fully deuterated blanks was also shown to be proportional to $(1 - T)$ with a constant of proportionality ~65% of that measured for hydrogenous blanks. Thus, the flat background scattering from labeled polymer samples apparently behaves similarly to that for H_2O/D_2O mixtures, and for the partially labeled samples the flat background was first estimated by scaling from the levels measured in the H and D blanks via the factor $\sigma_{inc}/\sigma_{tot}$, which has been shown to be appropriate for H_2O/D_2O mixtures. The intermediate-angle results using this method of background subtraction are shown in Figure 4 in the form of Kratky plots $(Q^2(d\Sigma/d\Omega)(Q)$ vs. $Q)$ for the three tacticities measured.

To check the sensitivity of these data to the method of background subtraction, we made alternative estimates of the flat background using methods developed by Hayashi et al.,[17] who assumed that the scattering from deuterated polymer blanks could be considered to be almost entirely coherent and that of H blanks predominantly incoherent. The H-blank scattering is proportional to $(1 - T_H)$, and $T_H \simeq \exp(-N\sigma_i t)$, where N is the number of protons per unit volume, t is the thickness, and σ_i is the hydrogen incoherent cross section. Thus for partially labeled samples the flat incoherent background may be scaled to $(1 - \exp(-N\sigma_i t))$ and the coherent background to the square of the average scattering length densities of the partially labeled sample and the D blank.[16-18] Figure 5 shows the Kratky plots for the data background corrected according

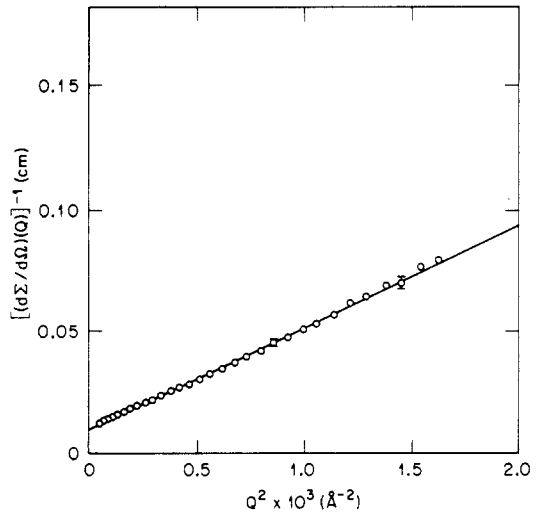

Figure 6. $[(d\Sigma/d\Omega)(Q)]^{-1}$ vs. Q^2 for 21.2 vol % PMMA-H molecules in a PMMA-D matrix. R_g^z = 107 Å; $(d\Sigma/d\Omega)(0)$ = 95.3 cm^{-1}.

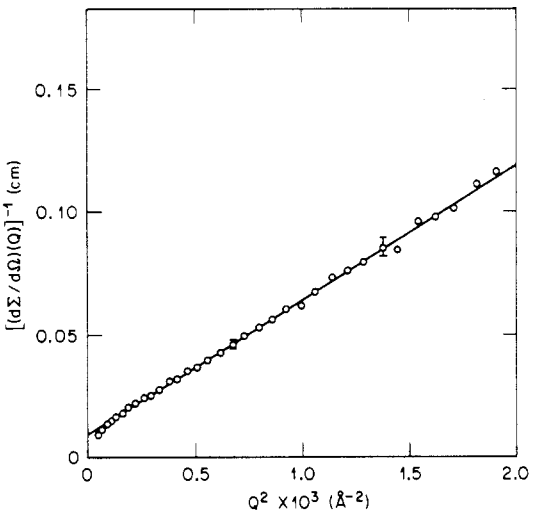

Figure 7. $[(d\Sigma/d\Omega)(Q)]^{-1}$ vs. Q^2 for 21.2 vol % isotactic PMMA-H molecules in a PMMA-D matrix. R_g^z = 127 Å; $(d\Sigma/d\Omega)(0)$ = 96.9 cm^{-1}.

to these methods; comparison with Figure 4 shows that the method of background subtraction does not introduce appreciable differences in the measured intermediate-angle scattering patterns. This is basically because a strong coherent signal has been obtained by using high levels of labeling (volume fraction of D polymer, $X \simeq 0.79$), which also minimizes the incoherent background. As the calculated background corrections are small with respect to the coherent signal, uncertainties in the background subtraction method do not appreciably affect the measured data.

Figure 6 shows the typical Zimm plot of the low-Q data for 21.2 vol % atactic PMMA-H molecules in a PMMA-D matrix. The plot is remarkably linear even in the Q range where QR_g exceeds unity ($QR_g \leq 4$), as has often been found for labeled polymer systems.[19] Some of the Zimm plots showed a slight change in slope below $Q \leq 0.01$ Å^{-1} (see Figure 7), presumably due to the presence of void scattering at low Q, which was present in some samples and blanks (see Figure 3). As the flat incoherent background corrections are virtually negligible in this Q range, some samples with predominantly hydrogenous matrices were made and measured. These samples, with an approximate H/D ratio of 8/2, had a lower average scattering length density and so were less sensitive to void scattering than the predominantly deuterated samples with a 2/8 H/D ratio. For all samples giving a change in slope at low Q, the data below $Q \leq 0.01$ were omitted when the data were fitted to a straight line according to[15,20]

$$\left[\frac{d\Sigma}{d\Omega}(Q)\right]^{-1} = \frac{1 + \Delta w(1 - X)}{C_N M_{wD}(1 + \Delta w)}\left[1 + \frac{Q^2 R_{g\,app}}{3}\right] \quad (1)$$

where $R_{g\,app}$ is an apparent radius of gyration related to the true (z averaged) radius of the labeled chains R_{gD} by

$$R_{g\,app} = R_{gD}\left[1 + \frac{X\Delta z}{1 + (1 - X)\Delta w}\right]^{1/2} \quad (2)$$

Δz and Δw depend on the mismatch of the weight-averaged (w) or z-averaged (z) polymerization indices (N) of the unlabeled (H) and labeled (D) chains as follows:

$$N_{wH} = N_{wD}(1 + \Delta w) \quad (3)$$

$$N_{zH} = N_{zD}(1 + \Delta z) \quad (4)$$

C_N is a constant given by

$$C_N = \frac{(a_H - a_D)^2 N_0 X(1 - X)\rho}{m_D^2} \quad (5)$$

where a_H and a_D are the coherent scattering lengths of the unlabeled and labeled repeat units, m_D is the mass of a D repeat unit, N_0 is Avogadro's number, ρ is the density, and X is the volume fraction of labeled (D) polymer. When the molecular weight distributions are approximately matched, the volume fraction X can be replaced by the mole fraction.[20]

Table I shows values of M_{wD} determined from light-scattering (LS) measurements. Using these values, we corrected the SANS data for mismatch (eq 1) and polydispersity[21] to yield the weight-averaged M_w and R_g for the D chains as shown in Table II. The molecular weights are the actual gram-molecular weights of the chain. There is generally good reproducibility between the R_g values measured in predominantly deuterated matrices (2/8 samples) and those measured in predominantly hydrogenous matrices (8/2 samples), indicating that the mismatch corrections have been correctly applied. The agreement between SANS and LS molecular weights is generally very good, and the values are within 3% for the isotactic and syndiotactic molecules. The maximum discrepancy occurs for the atactic polymers, though the difference (~13%) is still within the overall uncertainty of the SANS and LS measurements.

Table III shows the value of the characteristic ratio C_∞ of the D molecules compared with rotational isomeric state (RIS) calculations[22] and measurements in tetrahydrofuran solutions.[23]

In calculations of C_∞, the molecular weight used was an average of the SANS and light-scattering values. For

Table II
Sample Characterization by SANS

	$M_w \times 10^{-3}$ [a]	R_g^z, Å
	H-8 Molecules	
isotactic	117	
atactic	117	
syndiotactic	81	
	D-8 Molecules	
isotactic	106	119,[b] 120,[b] 116,[b] 119,[c] 116[c]
atactic	114	102,[b] 101,[b] 102,[b] 102,[c] 103[c]
syndiotactic	89	94,[c] 93[c]

[a] Average over several values from different samples. [b] Individual R_g from predominantly H sample (8/2 series). [c] Individual R_g from predominantly D sample (2/8 series).

Table III
Observed and Calculated Values of $(R_g^w/M_w^{1/2})$ and the Characteristic Ratio C_∞ for Bulk PMMA and Θ-Solvent

bulk PMMA	$R_g^w/M_w^{1/2}$, Å	C_∞(obsd), (SANS)	C_∞(obsd)[a]	C_∞(calcd)[b]
atactic (this work)	0.250	7.9	7.5	9.5
syndiotactic (this work)	0.270	9.2	7.3	7.5
isotactic (this work)	0.291	10.7	10.2	10.3
atactic[c]	0.26	8.5		

[a] Reference 23. [b] Reference 22. [c] Reference 1.

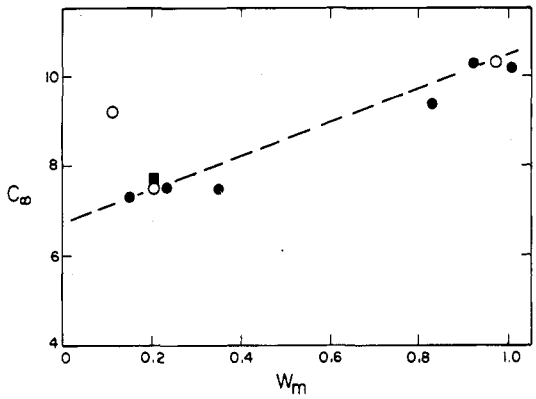

Figure 8. Characteristic ratio vs. weight fraction of meso diads: (○) SANS (this work); (●) ref 23; (■) ref 1.

isotactic PMMA, C_∞ from SANS, solution measurements, and calculations are in good agreement. For atactic PMMA, the SANS and solution measurements agree but are lower than the calculated value. For syndiotactic PMMA, the SANS measurements are higher than the solution and calculated values, which are in good accord. There is some evidence in the different solution measurements that C_∞ decreases as w_m, the fraction of isotactic placements, increases at low w_m and then increases at high w_m (see Figure 8, ref 22c). According to the calculations of Sundararajan and Flory, the dependence of C_∞ on w_m is a function of the conformational energies, E_α and E_β. The values of $E_\alpha = 1.2$ and $E_\beta = -0.2$ kcal/mol appear to be the most consistent with all of the data. The SANS data indicate that C_∞ for syndiotactic PMMA is greater than C_∞ for atactic PMMA, but both are within 8.5 ± 0.7, which is within the experimental uncertainty. The shapes of the intermediate-angle data are qualitatively as predicted by the RIS model. Figure 9 shows a comparison of the experimental data with RIS calculations[22] for polymers of similar tacticities. Within the overall uncertainties of the experiments and the RIS calculations, it appears that both the overall molecular conformation, as measured by R_g and C_∞, and the local chain conformation, as measured by the intermediate-angle data, seem to be described by the RIS for isotactic and atactic chains. No features in the scattering curves suggest substantial local order, which has been the subject of extensive speculation.[24] It would be interesting to repeat the RIS calculations for the tacticities that correspond to the PMMA molecules studied in this work (Table I). Earlier RIS calculations[22b] show an increase in scattering function with increasing Q for syndiotactic PMMA, but neither the SANS results nor the later calculations seem to follow this trend.

In the current RIS model of PMMA, the side-chain conformation is fixed (CH_3 cis to C=O). Spectroscopic results[9,26] and mechanical and dielectric relaxation[27] in PMMA indicate a multiplicity of side-chain states. We suggest that side-chain conformations should be included

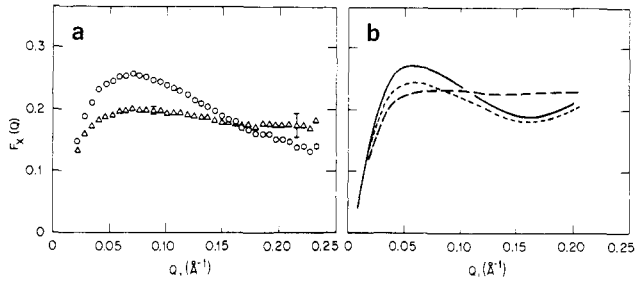

Figure 9. Absolute Kratky functions for PMMA with different tacticities (X_m = % meso-diad fraction). (a) (●) Syndiotactic, $X_m = 0.11$; (■) atactic, $X_m = 0.20$; (▲) isotactic, $X_m = 0.97$. (b) RIS calculations (ref 22).

in future RIS and scattering-function calculations. Recent IANS data on atactic PMMA by Dettenmaier et al.[28] give a peak level of the Kratky plot that reaches the plateau level for a Gaussian coil. Although the units or background corrections are not specified by Dettenmaier, we can calculate the Gaussian coil plateau level, which equals $2(d\Sigma(0)/d\Omega)/R_g^2$. As $d\Sigma(0)/d\Omega$ is proportional to the molecular weight, the plateau level can be calculated for a given ratio of M_w/R_g^2. Under the assumption of a value of $R_g/M_w^{1/2} = 0.26 \pm 0.01$ Å $g^{-1/2}$, this would imply a plateau level of 0.025 ± 0.002 $cm^{-1}/Å^2$. Thus the data of Figures 4 and 5 seem to be reasonably consistent with the results of Dettenmaier et al.[29]

Conclusions

The SANS results are generally consistent with the RIS predictions. Collectively, the spectroscopic,[9,26] thermodynamic,[25] and scattering measurements are self-consistent and delineate the conformational changes with tacticity in PMMA.

Acknowledgment. We are grateful to Dr. A. Leslie Stanford and Du Pont for samples of atactic PMMA-d_8 and methyl methacrylate monomer (d_8). We also thank Dr. Samuel Kaplan for obtaining NMR spectra and L. W. Fisher for the light-scattering data. This work was supported in part by a grant to D.M.T. from the National Science Foundation, No. SPI-7916618. The National Center for Small-Angle Scattering Research, Oak Ridge National Laboratory, is funded by National Science Foundation Grant No. DMO-77-467 through Interagency Agreement No. 40-637-77 with the Department of Energy (DOE) and is operated by the Martin Marietta Corp. under Contract No. DEA CO5840R 21400 with the DOE.

Registry No. atactic-PMMA (homopolymer), 9011-14-7; isotactic-PMMA (homopolymer), 25188-98-1; syndiotactic-PMMA (homopolymer), 25188-97-0; neutron, 12586-31-1.

References and Notes

(1) Kirste, R. G.; Kruse, W. A.; Schelten, J. *Makromol. Chem.* **1972**, *162*, 229.
(2) Benoit, H.; Cotton, J. P.; Decker, D.; Farnoux, B.; Higgins, J. S.; Jannink, G.; Ober, R.; Picot, C. *Nature (London)* **1973**, *245*, 13.
(3) Wignall, G. D.; Ballard, D. G. H.; Schelten, J. *Eur. Polym. J.* **1973**, *9*, 965; **1974**, *10*, 861.
(4) Schelten, J.; Wignall, G. D.; Ballard, D. G. H. *Polymer* **1974**, *15*, 682; **1976**, *17*, 751; **1977**, *18*, 1111.
(5) Lieser, G.; Fischer, E. W.; Ibel, K. *J. Polym. Sci.* **1975**, *13*, 39.
(6) Richards, R. W.; Maconnachie, A. *Polymer* **1978**, *19*, 739.
(7) Higgins, J. S.; Stein, R. S. *J. Appl. Crystallogr.* **1978**, *11*, 346.
(8) O'Reilly, J. M.; Stein, R. S.; Hadziioannou, G. P.; Wignall, G. D. *Polymer* **1983**, *24*, 1255.
(9) O'Reilly, J. M.; Teegarden, D. M.; Mosher, R. A. *Macromolecules* **1981**, *14*, 602, 1693.
(10) Jenkins, R.; Porter, R. *J. Polym. Sci., Polym. Lett. Ed.* **1980**, *18*, 743.
(11) Koehler, W. C.; Hendricks, R. W.; Child, H. R.; King, S. P.; Lin, J. S.; Wignall, G. D. "Scattering Techniques Applied to

Supramolecular and Nonequilibrium Systems"; Plenum: New York, 1981; p 75.
(12) Jacrot, B. *Rep. Prog. Phys.* **1976**, *39*, 911.
(13) Wignall, G. D.; Hendricks, R. W.; Koehler, W. C.; Lin, J. S.; Wai, M. P.; Thomas, E. L.; Stein, R. S. *Polymer* **1981**, *22*, 886.
(14) Hendricks, R. W.; Schelten, J.; Schmatz, W. *Philos. Mag.* **1974**, *30*, 819.
(15) Boue, F.; Nierlich, M.; Leibler, L. *Polymer* **1982**, *23*, 29.
(16) May, R. P.; Ibel, K.; Haas, J. *J. Appl. Crystallogr.* **1982**, *15*, 15.
(17) Hayashi, H.; Flory, P. J.; Wignall, G. D. *Macromolecules* **1983**, *16*, 1328.
(18) Akcasu, A. Z.; Summerfield, G. C.; Jahshan, S. N.; Han, C. C.; Kim, C. U.; Yu, H. *J. Polym. Sci.* **1980**, *18*, 865.
(19) Ballard, D. G. H.; Cheshire, P.; Janke, E.; Nevin, A.; Schelten, J. *Polymer* **1982**, *23*, 1875.
(20) Crist, B. W.; Graessley, W. W.; Wignall, G. D. *Polymer* **1982**, *23*, 1561.
(21) Altgelt, K.; Schultz, G. V. *Makromol. Chem.* **1960**, *36*, 209.
(22) (a) Yoon, D. Y.; Flory, P. J. *Polymer* **1975**, *16*, 645. (b) Yoon, D. Y.; Flory, P. J. *Macromolecules* **1976**, *9*, 299. (c) Sundararajan, P. R.; Flory, P. J. *J. Am. Chem. Soc.* **1974**, *96*, 5025.
(23) Jenkins, R.; Porter, R. *Polymer* **1983**, *23*, 105.
(24) Wendorff, J. H. *Polymer* **1982**, *23*, 543.
(25) O'Reilly, J. M.; Bair, H. E.; Karasz, F. E. *Macromolecules* **1982**, *15*, 1083.
(26) O'Reilly, J. M.; Mosher, R. A. *Macromolecules* **1981**, *14*, 602.
(27) McCrum, N. G.; Read, B. E.; Williams, G. "Anelastic and Dielectric Effects in Polymers"; Wiley: New York, 1967; p 245.
(28) Dettenmaier, M.; Maconnachie, A.; Higgins, J. S.; Kausch, H. H.; Nguyen, T. Q. *Macromolecules*, in press.

A Mean-Field Theory of Suspension Viscosity

Andrzej R. Altenberger and John S. Dahler*

Departments of Chemistry and Chemical Engineering, University of Minnesota, Minneapolis, Minnesota 55455

Matthew V. Tirrell

Department of Chemical Engineering and Materials Science, University of Minnesota, Minneapolis, Minnesota 55455. *Received April 4, 1985*

ABSTRACT: Hydrodynamic scattering theory is used to calculate the effective viscosity of a fluid through which spherical scattering centers are randomly dispersed. When the spheres are free to move, the system is a suspension. When the spheres are immobile, they mimic a porous medium. Calculations are performed for an arbitrary slip boundary condition at the fluid–sphere interface.

1. Introduction

A mean-field theory is proposed for the effective viscosity of a fluid permeated by a random distribution of spherical particles, freely suspended in one case and immobilized in another. Our approach is based on hydrodynamic multiple scattering theory. Calculations are performed for an arbitrary slip boundary condition at the fluid–sphere interface. We believe that the technique presented here is more straightforward and physically appealing than that which previously has been used.

In section 2 the Einstein suspension problem is analyzed from the point of view of hydrodynamic scattering theory. Section 3 is devoted to the problem of flow through a randomly distributed array of stationary obstacles, a model that often has been used for porous media.

2. The Suspension

We consider a stationary, incompressible flow perturbed by the presence of a single sphere of radius a, which is permitted to translate and rotate freely in the surrounding Newtonian fluid. The position vector of this sphere will be denoted by the symbol $\mathbf{R}$ and that of an arbitrary field point by $\mathbf{r}$. $\rho = \mathbf{r} - \mathbf{R}$ is the vector extending from the center of the sphere to the field point. The perturbation of the velocity field appropriate to an arbitrary slip boundary condition is given by the expression (for example, see p 249 of Batchelor[1])

$$\delta\mathbf{w}(\rho|\mathbf{R}) = -\frac{1-\lambda}{1+2\lambda}\frac{5}{2}\frac{a^3}{\rho^2}\hat{\rho}\hat{\rho}\cdot\underline{\underline{\alpha}}^{\circ}{}_S(\mathbf{R})\cdot\hat{\rho} - \frac{1-3\lambda}{1+2\lambda}\frac{a^5}{\rho^4}\left[\underline{\underline{\alpha}}^{\circ}{}_S(\mathbf{R})\cdot\hat{\rho} - \frac{5}{2}\hat{\rho}\hat{\rho}\cdot\underline{\underline{\alpha}}^{\circ}{}_S(\mathbf{R})\cdot\hat{\rho}\right] \quad (2.1)$$

provided that $|\rho| \geq a$. Here $\hat{\rho}$ is the unit vector $\rho/|\rho|$. The value of the slip coefficient λ can vary from $\lambda = 0$ for the stick boundary condition at the surface of the sphere to $\lambda = 1/3$ for perfect slip. The symbol $\alpha^{\circ}{}_S(\mathbf{R})$ appearing in eq 1 is the symmetric rate of strain tensor associated with the original unperturbed flow $\mathbf{w}^{\circ}(\mathbf{R})$, viz.

$$[\underline{\underline{\alpha}}^{\circ}{}_S(\mathbf{R})]_{ij} = \tfrac{1}{2}[\partial w^{\circ}{}_i/\partial X_j + \partial w^{\circ}{}_j/\partial X_i] \quad (2.2)$$

with X_i denoting a Cartesian component of $\mathbf{R}$. Strictly speaking, the formula 2.1 is valiid only if the rate of strain varies negligibly over distances comparable to the size of the sphere, i.e., only if $\alpha^{\circ}{}_S(\mathbf{R} + \mathbf{a}) \approx \alpha^{\circ}{}_S(\mathbf{R})$.

We now rewrite the perturbation $\delta\bar{\mathbf{w}}(\rho|\mathbf{R})$ in the form $\underline{\underline{\underline{B}}}(\rho)$: $\nabla_R\mathbf{w}^{\circ}(\mathbf{R})$ with $\underline{\underline{\underline{B}}}(\rho)$ the third-rank tensor defined (for $|\rho| \geq a$) by the formula

$$\underline{\underline{\underline{B}}}(\rho) = -\frac{1-\lambda}{1+2\lambda}\frac{5a^3}{2}\left(\frac{1}{\rho^2}\hat{\rho}\hat{\rho}\hat{\rho}\right) - \frac{1-3\lambda}{1+2\lambda}\frac{a^5}{2}\nabla_\rho\left(\frac{1}{\rho^3}\hat{\rho}\hat{\rho}\right) \quad (2.3)$$

The fluid velocity at the location $\mathbf{r}$ is then given by the expression

$$\mathbf{w}(\mathbf{r};\mathbf{R}) = \mathbf{w}^{\circ}(\mathbf{r}) + \underline{\underline{\underline{B}}}(\mathbf{r} - \mathbf{R}):\ \nabla_R\mathbf{w}^{\circ}(\mathbf{R}) \quad (2.4)$$

Because the interior of the sphere is not accessible to the fluid, eq 2.4 is applicable only if $|\mathbf{r} - \mathbf{R}| \geq a$.

The relation 2.4 provides a specific example of a more general rule of hydrodynamic scattering theory, according to which, for an arbitrary unperturbed flow $\mathbf{w}^{\circ}(\mathbf{R})$ and for an arbitrary boundary condition on the surface of the target, there exists a linear functional relationship between the "incoming" (unperturbed) flow and the perturbation $\delta\mathbf{w}$ resulting from the presence of the target. This relationship can be expressed in the form

0024-9297/85/2218-2752$01.50/0 © 1985 American Chemical Society